

# Magnetic Investigations on a Valence-Delocalized Dinuclear Fe(II)-Fe(III) Complex

C. Saal<sup>1</sup>), S. Mohanta<sup>2</sup>), K. Nag<sup>2</sup>), S.K. Dutta<sup>2</sup>), R. Werner<sup>1</sup>), W. Haase<sup>1</sup>), E. Duin<sup>3</sup>), and M.K. Johnson<sup>3</sup>)

<sup>1</sup>) Institut für Physikalische Chemie, TH Darmstadt, Petersenstraße 20, D-64287 Darmstadt, Germany

<sup>2</sup>) Department of Inorganic Chemistry, Indian Association for the Cultivation of Science, Jadavpur, Calcutta 700032, India

<sup>3</sup>) Department of Chemistry, University of Georgia, Athens, GA 30602, USA

**Key Words:** Complex Compounds / Magnetism / Valence Delocalisation

The magnetic properties of a valence delocalized mixed valent Fe(II)-Fe(III) complex have been investigated. On the basis of magnetic susceptibility measurements and NIR absorption spectroscopy the double exchange parameter was determined to  $B = 940 \text{ cm}^{-1}$  while for the isotropic exchange interaction an antiferromagnetic contribution of  $J = -100 \text{ cm}^{-1}$  was obtained. The results were further discussed with regard to vibronic interaction.

For the vibronic-interaction parameter  $\lambda$  only an upper bound of  $2500 \text{ cm}^{-1}$  could be given.

## Introduction

Polynuclear transition metal compounds with metal centers in different oxidation states are of potential interest since these systems exhibit the possibility to study the intramolecular electron transfer. Such systems are not only models to investigate the mechanism of valence trapping or valence delocalization but are also present in biological systems. The tetrameric manganese unit in photosystem II perhaps represents the most famous example of mixed valence systems in biology.

To gain some insight in the magnetic effects of the electron transfer it is easier to study model complexes containing as few as possible spin-centers. Of great interest was the preparation by Creutz and Taube of the  $\mu$ -pyrazine-bis(pentaamminruthenium) (5+) ion [1, 2]. The investigation of mixed valent iron complexes allows to draw additional informations from Mössbauer investigations. The first example of a valence delocalized, dimeric Fe(II)-Fe(III) complex of class III in the Robin Day classification was  $[\text{L}_2\text{Fe}_2(\mu\text{-OH})_3]^{2+}$  which was prepared by Wiegardt et al. [3, 4]. This complex was studied in detail by Mössbauer- and EPR-spectroscopy. Unfortunately the determination of the double exchange parameter  $B$  and the exchange parameter  $J$  is not possible with high accuracy using these techniques. Measurements of the magnetic susceptibility and investigation of the intervalence band seem to be more suitable for the determination of these parameters.

Here we report a detailed analysis of the temperature dependence of the magnetic susceptibility of a new Fe(II)-Fe(III)-dimer (Fig. 1) which was claimed to be valence delocalized on the basis of Mössbauer investigations [5].

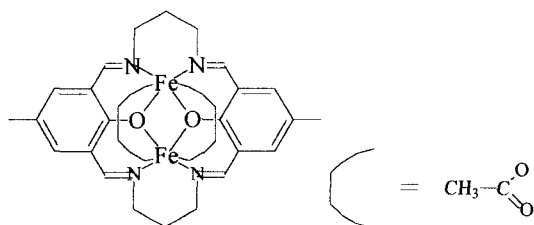


Fig. 1  
Structure of  $[\text{L}^1\text{Fe}_2(\mu\text{-OAc})_2]^+$

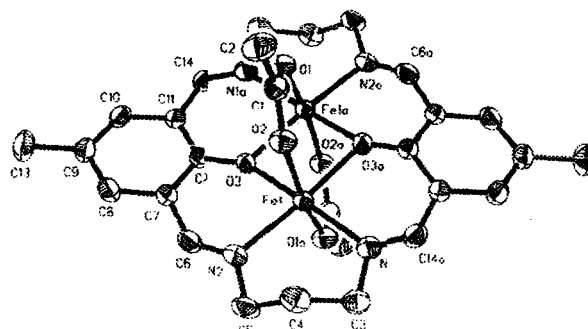
## Experiment

The synthesis of  $[\text{L}^1\text{Fe}_2(\mu\text{-OAc})_2](\text{ClO}_4)$  is described elsewhere [5]. Temperature dependent measurements of the magnetic susceptibility in the temperature range 4.8 – 260 K were carried out using a Faraday balance [6].  $\text{Hg}[\text{Co}(\text{NCS})_4]$  was used as a calibration standard. Diamagnetic corrections were made using Pascal's constants. The temperature independent paramagnetism was fixed to  $400 \cdot 10^{-6} \text{ cm}^3 \text{ mol}^{-1}$ . Because the powdered sample was strongly oriented by the magnetic field the sample was immersed in paraffin (Merck) and cooled down to liquid helium temperature in zero field. The measurement was performed from low temperatures towards higher temperatures. The diamagnetic correction for the paraffin was obtained by measuring the magnetic susceptibility of the paraffin in dependence of temperature. This susceptibility proved to be temperature independent.

To calculate magnetic susceptibility on the basis of a given set of parameters we used matrix-diagonalisation.

## Results and Discussion

The crystal structure of the complex is described in detail elsewhere [5]. The ORTEP-plot of the cation is shown in Fig. 2. The structure consists of two macrocyclic  $\text{FeO}_2\text{N}_2$  coordination cores linked by two phenoxo groups which



leads to edge sharing between two  $\text{FeO}_4\text{N}_2$  octahedra. The Fe-Fe distance is 2.741 Å. For the first coordination sphere of the iron ions we obtained the following interatomic distances: Fe-O (phenoxo) = 2.033 Å, Fe-O (acetate) = 2.055 Å and Fe-N = 2.141 Å. The cation possesses a center of inversion leading to equivalent positions for the two iron ions.

The magnetic susceptibility and the effective magnetic moment are plotted in Fig. 3 versus temperature. Above 265 K we observed a sudden increase of the magnetic moment which is due to the fact that the paraffin melts at this temperature and orientation of the crystals occurs.

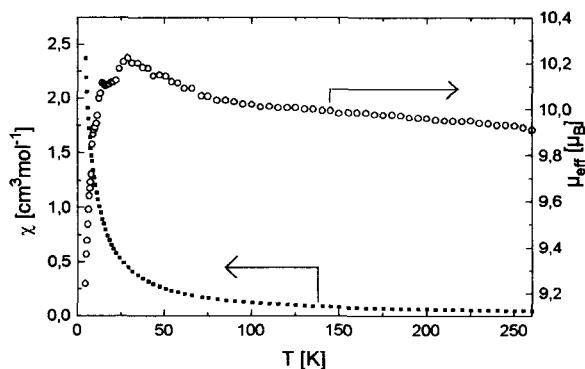


Fig. 3 Molar magnetic susceptibility and effective magnetic moment data versus temperature for  $[\text{L}^1\text{Fe}_2(\mu\text{-OAc})_2](\text{ClO}_4)$

The effective magnetic moment increases in the temperature range 30–265 K towards lower temperatures. The increase becomes steeper below 70 K. At 30 K we observe a maximum value of  $10.2 \mu_B$  for the effective magnetic moment which indicates a  $S = 9/2$  ground state. Below this temperature we observed a rapid decrease of the effective magnetic moment. The value at 265 K is  $9.9 \mu_B$  gives a hint that at this temperature the ground state is still the only multiplet which is considerably populated.

To analyse the observed behaviour we used the following general Hamiltonian which was simplified to reduce the number of parameters:

$$\begin{aligned} \hat{H} = & -J({}^A\hat{S}_1 {}^A\hat{S}_2 \hat{O}_A + {}^B\hat{S}_1 {}^B\hat{S}_2 \hat{O}_B) + \hat{T} \\ & + \mu_B \hat{H} \tilde{g} [({}^A\hat{S}_1 + {}^A\hat{S}_2) \hat{O}_A + ({}^B\hat{S}_1 + {}^B\hat{S}_2) \hat{O}_B] \\ & + D_1 [\hat{S}_{1z}^2 - \frac{1}{3} S_1(S_1 + 1)] + D_2 [\hat{S}_{2z}^2 - \frac{1}{3} S_2(S_2 + 1)] \\ & + E_1 [\hat{S}_{1x}^2 - \hat{S}_{1y}^2] + E_2 [\hat{S}_{2x}^2 - \hat{S}_{2y}^2] + zJ\langle S_z \rangle \hat{S}_z + \hat{O}_{\text{vib}} \end{aligned}$$

The first part of this Hamiltonian is due to the isotropic exchange interaction and takes into account the fact that one electron is delocalized over the two iron ions by introduction of the occupation operators  $\hat{O}_A$  and  $\hat{O}_B$ . A and B denote the configurations  ${}^A\text{Fe(II)}\text{-}{}^B\text{Fe(III)}$  and  ${}^A\text{Fe(III)}\text{-}{}^B\text{Fe(II)}$  with the extra electron on center A or B. The effect of this operator is given by the following relations:

$$\hat{O}_A |A, S, M_S\rangle = |A, S, M_S\rangle \quad \hat{O}_A |B, S, M_S\rangle = 0$$

Similar expressions result by permuting A and B. The double exchange-operator  $\hat{T}$  describes the interaction of the system in spin-state  $S$  with the excess electron on center A with the system with excess electron on center B. It also takes into account that the effect of intramolecular electron transfer is spin-dependent [7]:

$$\hat{T} |A, S, M_S\rangle = B(S + 1/2) |B, S, M_S\rangle$$

$$\hat{T} |B, S, M_S\rangle = B(S + 1/2) |A, S, M_S\rangle$$

The third term describes the Zeeman-interaction. The two following terms introduce the axial and non-axial zero-field splitting. (To avoid a lengthy formula for the ZFS-part of the spin Hamiltonian above only one configuration is considered in the Hamiltonian but for calculations both were used.) When a spin multiplet is separated from adjacent spin states by energy gaps of an order of magnitude larger than the zero-field interaction, the zero-field interaction for the spin-multiplets with higher energy is negligible. Consequently in our case only the zero-field splitting of the  $S = 9/2$  ground state should have remarkable effects on the magnetic susceptibility. Also the existence of a ferromagnetic intercluster interaction described by the second last term in the spin Hamiltonian complicates the determination of  $|D\rangle$  and  $|E\rangle$ . For the calculation of the matrix elements of the zero-field-splitting terms we used instead of the basis functions  $|{}^iS_1, {}^iS_2, S, M\rangle$  the set of functions for the uncoupled iron ions  $|{}^iS_1, M_1, {}^iS_2, M_2\rangle$  which is connected to the first one by the Clebsch-Gordon coefficients:

$$\begin{aligned} |{}^iS_1, {}^iS_2, S, M\rangle = & \sum_{M_1, M_2} |{}^iS_1, M_1, {}^iS_2, M_2\rangle \\ & \cdot \langle {}^iS_1, M_1, {}^iS_2, M_2 | {}^iS_1, {}^iS_2, S, M \rangle \quad i = A, B \end{aligned}$$

Using this relation the matrix elements were calculated according to:

$$\begin{aligned} \langle {}^iS_1, {}^iS_2, S, M | \hat{O} | {}^iS_1, {}^iS_2, S', M' \rangle \\ = \sum_{M_1, M_2} \langle {}^iS_1, M_1, {}^iS_2, M_2 | {}^iS_1, {}^iS_2, S, M \rangle \\ \cdot \langle {}^iS_1, M_1, {}^iS_2, M_2 | {}^iS_1, {}^iS_2, S', M' \rangle \\ \cdot \langle {}^iS_1, M_1, {}^iS_2, M_2 | \hat{O} | {}^iS_1, M_1, {}^iS_2, M_2 \rangle \quad i = A, B \end{aligned}$$

Because the zero-field-terms in the Hamiltonian do not lead to matrix elements connecting states with the extra electron on  ${}^A\text{Fe}$  and  ${}^B\text{Fe}$  the labels A and B were omitted in the last two lines of the equation for  $\hat{H}$ .

The last term in the Hamiltonian is used to describe the vibronic interaction. This term was introduced by Wong and Schatz [8] and will be discussed later.

In the “high temperature” range (above 30 K) the temperature dependence of the effective magnetic moment can be explained by considering only double-exchange and super-exchange in the Hamiltonian given above. In this case the eigenvalues of the spin-Hamiltonian can easily be found by

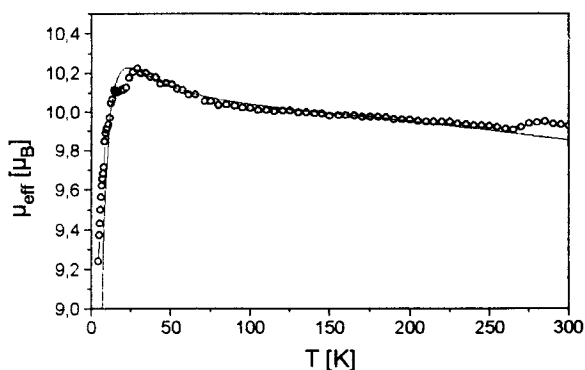


Fig. 4

Effective magnetic moment of  $[L^1Fe_2(\mu-OAc)_2](ClO_4)$ . The open circles represent the experimental values, the solid lines represent the best fit obtained with  $J = -100 \text{ cm}^{-1}$ ,  $B = 940 \text{ cm}^{-1}$ ,  $g = 2.00$ ,  $x_p = 0.03$ ,  $zJ = 0.45$ ,  $|D| = 1.6 \text{ cm}^{-1}$  and  $|E| = 0.27 \text{ cm}^{-1}$ .  $\chi_x$  and  $\chi_z$  were calculated and the effective magnetic moment was calculated as  $\mu_{\text{eff}}/\mu_B = 2.828 \cdot \sqrt{\chi T}$  where  $\chi = (\chi_z + 2\chi_x)/3$

analytical methods [9]. We obtained fits of the same quality with different sets of  $J$  and  $B$  and  $g = 2.00$ ,  $x_p = 0.03$  and  $zJ = 0.45$  (Fig. 4). The steeper increase of the effective magnetic moment towards lower temperature in the range 30–70 K is due to the ferromagnetic intercluster interaction described by the last parameter  $zJ$  which gives a considerably weaker interaction than the intramolecular coupling. For the double-exchange parameter  $B$  and the isotropic coupling constant  $J$  we found a linear relationship shown in Fig. 5. This is due to the fact that the temperature dependence of the magnetic susceptibility is influenced only by the population of the two lowest spin states ( $S = 9/2$  and  $S = 7/2$ ) and this energy gap is determined by a linear combination of both parameters. To fix  $J$  and  $B$  it is necessary that at least one more spin state is considerably populated or to use spectroscopic techniques. From the position of the intervalence band at 1060 nm the double exchange parameter can be estimated to  $940 \text{ cm}^{-1}$  which leads to  $J = -100 \text{ cm}^{-1}$ . The population of the lower five spin

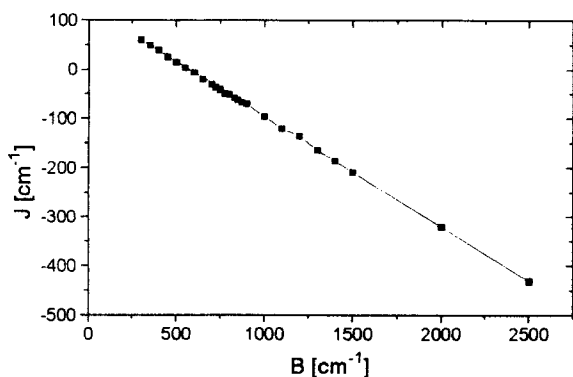


Fig. 5

Linear dependence of the isotropic exchange parameter  $J$  and the double exchange parameter  $B$

states versus temperature is plotted in Fig. 6. It can be seen that even at room temperature the population of the  $S = 5/2$  state is only 0.1%. The “low temperature” behaviour (below 30 K) is strongly affected from the zero-field-splitting of the  $S = 9/2$  state. The axial zero-field-splitting of this spin-state can – as well as the non-axial zero-field splitting – be described using only one parameter. Consequently it is not possible to determine  $D_1$  and  $D_2$  (or  $E_1$  and  $E_2$ ) separately. The zero-field-splitting parameters for the other spin states can be expressed as spin-dependent linear combinations of the zero-field-splitting parameters for Fe(II) and Fe(III) and therefore it is only possible to determine all of them if the energy gap between the two lowest multiplets is in the same order of magnitude as the zero-field splitting. From our measurement we obtained the values of the cluster zero-field-splitting parameters – as defined in [4] –  $|D| = 1.6 \text{ cm}^{-1}$  and  $|E| = 0.27 \text{ cm}^{-1}$ . The ratio  $E/D$  was fixed to 0.17 which is known from EPR-experiments [12]. The determination of  $|D|$  and  $|E|$  from magnetic susceptibility measurements can only be considered as a rough estimate because of the influence of the ferromagnetic intercluster-interaction for which  $zJ$  is only a very crude description.

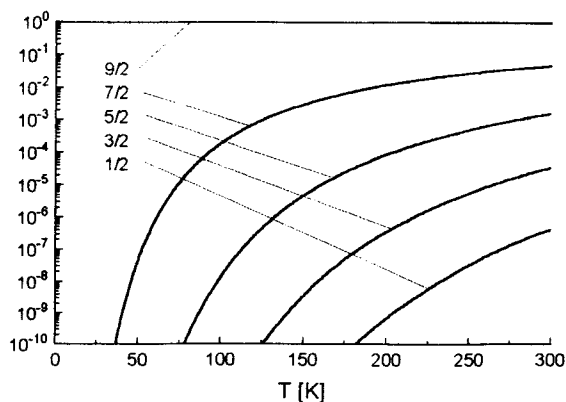


Fig. 6

Relative population of the lowest five multiplets as function of the temperature calculated for  $J = -100 \text{ cm}^{-1}$  and  $B = 940 \text{ cm}^{-1}$

According to the PKS (Piepho, Krausz, Schatz)-model [8] the magnetic susceptibility should be influenced by a vibronic coupling because the antisymmetric combination of the “breathing-mode” of the two octahedrally coordinated Fe-ions should have an effect on the electron transfer between them. This effect was also discussed by other authors [10, 11]. Taking into account the vibronic coupling leads to one potential-curve for each spin-multiplet. The vibronic interaction was introduced by:

$$\hat{O}_{\text{vib}} = \pm \frac{1}{\sqrt{2}} \lambda Q_- + \frac{1}{2} \lambda Q_-^2$$

This part of the spin Hamiltonian leads only to diagonal terms and we obtain as eigenvalues:

$$U_{\pm}^{(S)}(Q_{-}) = -JS(S+1) + \frac{1}{2}\lambda Q_{-}^2 \pm \sqrt{B^2 \frac{(S+1/2)^2}{(2S_0+1)^2} + \frac{1}{2}\lambda^2 Q_{-}^2}$$

Potential-curves for our  $d^5-d^6$ -system are shown in Fig. 7. To take into account the vibronic interaction in the calculation of the magnetic susceptibility we have to add up the contributions from all spin states and to integrate for each spin state over  $Q_{-}$ :

$$\chi(T) = N_A \frac{g^2 \mu_B^2}{3kT}$$

$$\frac{\sum_S S(S+1)(2S+1) \sum_{i=+,-} \int_{-\infty}^{+\infty} \exp[-U_i^{(S)}(Q_{-})/kT] dQ_{-}}{\sum_S (2S+1) \sum_{i=+,-} \int_{-\infty}^{+\infty} \exp[-U_i^{(S)}(Q_{-})/kT] dQ_{-}}$$

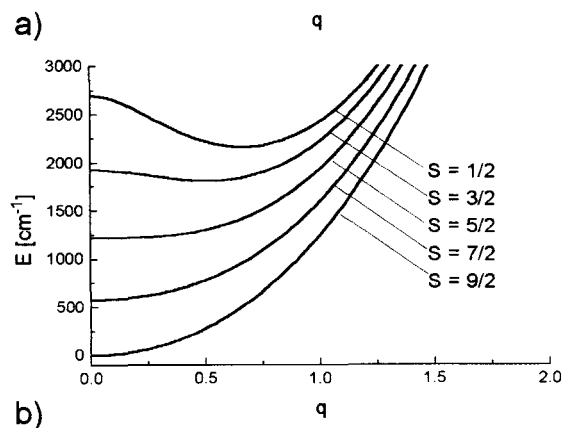
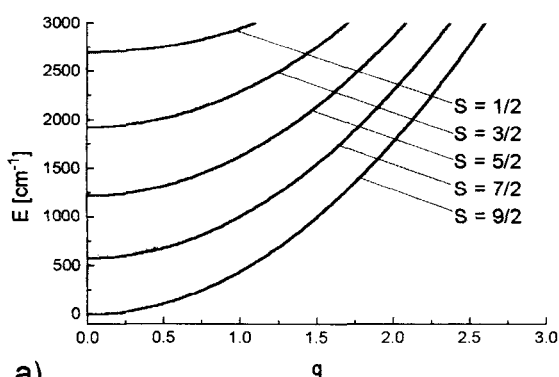


Fig. 7 Potential curves for the  $d^5-d^6$  system with  $J = -100 \text{ cm}^{-1}$ ,  $B = 940 \text{ cm}^{-1}$  and a)  $\lambda = 1000 \text{ cm}^{-1}$ , b)  $\lambda = 5000 \text{ cm}^{-1}$

The integration for each temperature was carried out for at least 100 points of the potential curves which were chosen equidistant in the range  $Q_{-} = 0$  to an upper limiting value. This upper limiting value was determined by

observing its influence on the calculated curve. When no effect on the theoretical values was observed on increasing the number of points and on increasing the upper limiting value this value was fixed.

In the case of a valence-delocalized dimer the potential curves possess a single minimum, while for a valence trapped compound a double minimum results. Consequently the behaviour of a valence trapped dimer may differ not only quantitatively but also qualitatively when described under consideration or neglect of the vibronic interaction. In this extreme extreme case one obtains ground states of different multiplicity for both cases.

For valence delocalized dimers the effect of vibronic coupling can not lead to a change in spin-multiplicity for the ground state but a quantitative effect is observed. In Fig. 8 the effective magnetic moment is plotted versus temperature for the parameters obtained by fitting the experimental data neglecting the vibronic interaction as described above. For the different curves the vibronic coupling parameter  $\lambda$  was varied in the range  $0.1 - 10000 \text{ cm}^{-1}$ . A considerable influence on the temperature dependence was only observed for  $\lambda > 2500 \text{ cm}^{-1}$ . The remaining curves are practically indistinguishable. Therefore it is only possible to determine an upper limiting value for the vibronic coupling parameter of  $2500 \text{ cm}^{-1}$ . The potential curves for  $\lambda = 1000 \text{ cm}^{-1}$  and  $\lambda = 5000 \text{ cm}^{-1}$  are shown in Fig. 7. In both cases single minima are obtained for the  $S = 9/2$ ,  $S = 7/2$  and  $S = 5/2$  state. Qualitative differences occur for the  $S = 3/2$  and  $S = 1/2$  state. While for  $\lambda = 1000 \text{ cm}^{-1}$  there is still a single minimum for the case  $\lambda = 5000 \text{ cm}^{-1}$  these states possess double minima. The presence of double minima for states of lower multiplicity reflects the fact that double exchange is most efficient for states with high quantum numbers of the total spin. Even for  $\lambda = 2500 \text{ cm}^{-1}$  the  $S = 1/2$  state has a double minimum structure, while all the other multiplets possess single minima. Consequently it is not possible to decide on the basis of the magnetic susceptibility data whether all of the potential curves of the dimer have the typical single-minimum structure of a valence delocalized compound because the states with  $S \leq 5/2$  are

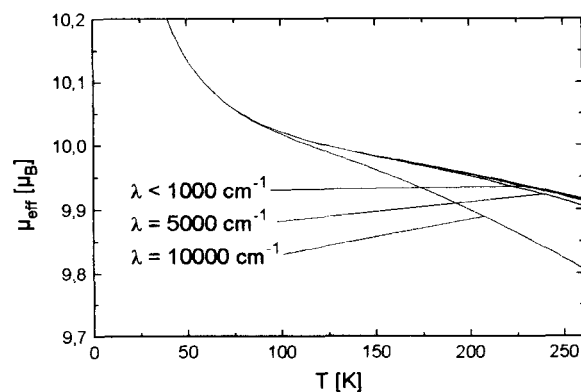


Fig. 8 Effective magnetic moment versus temperature for different vibronic coupling parameters ( $J = -100 \text{ cm}^{-1}$ ,  $B = 940 \text{ cm}^{-1}$ ,  $\lambda < 1000 \text{ cm}^{-1}$ ,  $\lambda = 5000 \text{ cm}^{-1}$  and  $\lambda = 10000 \text{ cm}^{-1}$ )

not thermal accessible. Even if the  $S = 1/2$  state has a double minimum this does not automatically lead to valence trapping because the  $S = 1/2$  potential barrier in the  $S = 1/2$  state is low compared to the difference in energy between the potential minimum of this multiplett and the ground state energy of the  $S = 9/2$  state.

### Conclusion

The double-exchange constant and isotropic exchange parameter for a dinuclear mixed-valent Fe(II)-Fe(III) complex which was considered to be valence delocalized on the basis of Moessbauer investigations have been determined. The double exchange seems to be the dominant interaction being stronger by a factor of 10 than the isotropic exchange interaction. Consequently we find a  $S = 9/2$  ground state and only the  $S = 7/2$  multiplet is considerably populated at room temperature. The remaining spin states are not thermal accessible at temperatures which don't lead to decomposition of the complex.

The effect of vibronic coupling on the mechanism of the valence delocalization was also investigated but a unique determination of the vibronic coupling parameter was not possible. Only an upper limiting value of  $2500 \text{ cm}^{-1}$  can be given. For the case of weak vibronic coupling we find single-minimum potential curves for all spin-states, while stronger vibronic coupling leads to the occurrence of double-minimum structures for the spin multiplets with lower spin momentum.

In comparison to the valence delocalized Fe(II)-Fe(III) dimeric complex by Wieghardt et al. [4] the double exchange parameter  $B$  is considerably smaller and we were able to give not only a lower bound for the isotropic exchange constant on the basis of the multiplicity of the ground state but also an estimate for it. This shows that in our case there is a ferromagnetic contributions from the double exchange and an antiferromagnetic contribution from the isotropic exchange.

The contribution of the antisymmetric combination of the "breathing mode" of two octahedrally coordinated ions was originally proposed by Piepho, Krausz and Schatz [8]. Calculations of magnetic susceptibility on the basis of this model were introduced by Tsukerbalt et al. [11]. However recently Solomon et al. [13] have shown by resonance-Raman studies that for valence-delocalized compounds also total-symmetric modes are involved in the valence delocalization.

### References

- [1] C. Creutz and H. Taube, *J. Am. Chem. Soc.* **91**, 3988 (1969).
- [2] C. Creutz and H. Taube, *J. Am. Chem. Soc.* **95**, 1086 (1973).
- [3] S. Drüeke, P. Chaudhuri, K. Pohl, K. Wieghardt, X.-Q. Ding, E. Bill, A. Sawaryn, A. X. Trautwein, H. Winkler, and S. J. Gurrmann, *J. Chem. Soc., Chem. Commun.* **59** (1989).
- [4] X.-Q. Ding, E. L. Bominaar, E. Bill, H. Winkler, A. X. Trautwein, S. Drüeke, P. Chaudhuri, and K. Wieghardt, *J. Chem. Phys.* **92**, 178 (1990).
- [5] S.K. Dutta, J. Ensling, R. Werner, U. Flörke, W. Haase, P. Gütllich, and K. Nag, *Angew. Chem.* submitted for publication.
- [6] S. Gehring, P. Fleischhauer, H. Paulus, and W. Haase, *Inorg. Chem.* **32**, 54 (1993).
- [7] P. W. Anderson and H. Hasegawa, *Phys. Rev.* **100**, 675 (1955).
- [8] K. Y. Wong and P. N. Schatz, *Prog. Inorg. Chem.* **369** (1981).
- [9] S. B. Piepho, E. R. Krausz, and P. N. Schatz, *J. Am. Chem. Soc.* **100**, 2996 (1978).
- [10] O. Kahn, "Molecular Magnetism", VCH Weinheim (1993).
- [11] J. J. Gired, *J. Chem. Phys.* **79**, 1766 (1983).
- [12] J. J. Borrás-Almenar, E. Coronado, B. S. Tsukerblat, and R. Georges, NATO ASI Series, Localized and Itinerant Molecular Magnetism, submitted for publication.
- [13] E. Duin and M. Johnson, unpublished results.
- [14] D. R. Gamelin, E. L. Bominaar, C. Mathonière, M. L. Kirk, K. Wieghardt, J.-J. Gired, and E. I. Solomon, *Inorg. Chem.* **35**, 4323 (1996).

Presented at the 95th Annual Meeting of the Deutsche Bunsen-Gesellschaft für Physikalische Chemie "Primärprozesse der Photosynthese" in Jena, May 16th to 18th, 1996 E 9370